HHS Public Access

Author manuscript

Nat Med. Author manuscript; available in PMC 2012 September 01.

Published in final edited form as:

Nat Med. ; 18(3): 436–440. doi:10.1038/nm.2610.

Reverse engineering of TLX oncogenic transcriptional networks identifies *RUNX1* as tumor suppressor in T-ALL

Giusy Della Gatta[1], **Teresa Palomero**[1,2], **Arianne Perez-Garcia**[1], **Alberto Ambesi-Impiombato**[1], **Mukesh Bansal**[3], **Zachary W. Carpenter**[1], **Kim De Keersmaecker**[4,5], **Xavier Sole**[6,7], **Luyao Xu**[1], **Elisabeth Paietta**[8,9], **Janis Racevskis**[8,9], **Peter H Wiernik**[8,9], **Jacob M Rowe**[10], **Jules P Meijerink**[11], **Andrea Califano**[1,3], and **Adolfo A. Ferrando**[1,2,12]

[1]Institute for Cancer Genetics, Columbia University, New York, NY, USA. [2]Department of Pathology, Columbia University Medical Center, New York, NY, USA. [3]Joint Centers for Systems Biology, Columbia University, New York, NY, USA. [4]Department of Molecular and Developmental Genetics, VIB, Leuven, Belgium. [5]Center for Human Genetics, K. U. Leuven, Leuven, Belgium. [6]Biomarkers and Susceptibility Unit, Catalan Institute of Oncology, IDIBELL, L'Hospitalet, Barcelona, Spain [7]Biomedical Research Centre Network for Epidemiology and Public Health, Catalan Institute of Oncology, IDIBELL, L'Hospitalet, Barcelona, Spain [8]Montefiore Medical Center North, New York, NY, USA. [9]New York Medical College, New York, NY, USA. [10]Rambam Medical Center and Technion, Israel Institute of Technology, Haifa, Israel. [11]Department of Pediatric Oncology/Hematology, Erasmus MC-Sophia Children's Hospital, Rotterdam, the Netherlands. [12]Department of Pediatrics, Columbia University Medical Center, New York, NY, USA.

Abstract

The *TLX1* and *TLX3* transcription factor oncogenes play an important role in the pathogenesis of T-cell acute lymphoblastic leukemia (T-ALL)[1,2]. Here we used reverse engineering of global transcriptional networks to decipher the oncogenic regulatory circuit controlled by *TLX1* and *TLX3*. This Systems Biology analysis defined TLX1 and TLX3 as master regulators of an oncogenic transcriptional circuit governing T-ALL. Notably, network structure analysis of this hierarchical network identified *RUNX1* as an important mediator of *TLX1* and *TLX3* induced T-ALL, and predicted a tumor suppressor role for *RUNX1* in T-cell transformation. Consistent with these results, we identified recurrent somatic loss of function mutations in *RUNX1* in human T-ALL. Overall, these results place *TLX1* and *TLX3* atop of an oncogenic transcriptional network controlling leukemia development, demonstrate power of network analysis to identify key elements in the regulatory circuits governing human cancer and identify *RUNX1* as a tumor suppressor gene in T-ALL.

Contact Information: Adolfo A. Ferrando Assistant Professor of Pediatrics and Pathology Institute for Cancer Genetics, Columbia University Medical Center 1130 St Nicholas Ave. ICRC-402A New York, NY, 10032 Phone: 212-851-4611 FAX: 212-851-5256 af2196@columbia.edu.

TLX1 and *TLX3* encode highly related homeobox transcription factor oncogenes frequently activated by chromosomal translocations in T-ALL [3-5].

To interrogate the transcriptional programs associated with aberrant expression of *TLX1* and *TLX3*, we analyzed gene expression data from 82 human T-ALLs [6]. This analysis revealed that *TLX1* and *TLX3* tumors share a common expression signature including 319 up-regulated and 450 down-regulated gene transcripts respectively (Fold change >2, $P < 0.005$) (Fig. 1a; Supplementary Table 1). Moreover, non negative matrix factorization (NMF) and Principal Component Analysis showed that TLX1 and TLX3 leukemias are highly related and clustered together separate from the rest of T-ALL samples in our series (Supplementary Figure 1). These results support a broadly overlapping role of TLX1 and TLX3 in the induction of T-ALL, however, TLX1 and TLX3 leukemias have been associated with different prognosis in some series [1,7], suggesting important biological differences between these two groups. Consistently, comparative marker analysis identified a broad gene expression signature in TLX1 T-ALLs compared with TLX3 tumors (Supplementary Figure 2).

Next, we analyzed TLX1 ChIP-chip data from ALL-SIL, a T-ALL cell line expressing high levels of *TLX1* as result of the t(10;14)(q24;q11) translocation[3] and performed ChIP-chip analysis for TLX3 in HPB-ALL, a t(5;14)(q35;q32) *TLX3*-activating translocation positive line[8]. These analyses identified 2,236 promoters bound by TLX1 and 3,148 promoters occupied by TLX3 with a significance cutoff of $P < 10^{-9}$ (Supplementary Table 2). Strikingly, 75% of TLX1 direct targets were also bound by TLX3 (Chi-square $P < 0.001$) (Fig. 1b). Finally, Gene Set Enrichment Analysis (GSEA) demonstrated a highly significant enrichment of genes whose promoter was bound by TLX1 and TLX3 in the expression signature associated with *TLX1* and *TLX3* leukemias ($P < 0.001$) (Fig. 1c) (Supplementary Table 3). Most notably, genes bound by *TLX1* and *TLX3* were characteristically downregulated in this group (Fig. 1c), strongly suggesting that *TLX1* and *TLX3* primarily function as transcriptional repressors in the pathogenesis of T-ALL.

We then used the ARACNe reverse-engineering algorithm[9,10] to generate a genome-wide T-ALL transcriptional network or T-ALL interactome (T-ALLi) using gene expression data from 228 T-ALLs. This analysis yielded a T-ALLi including 19,689 genes (nodes) connected via 471,824 interactions (edges) (Supplementary Figure 3). Notably, MYC target genes inferred in the T-ALLi were markedly enriched in MYC ChIP-chip direct target genes (74/252, Chi-square $P = 2.5\times10^{-5}$) supporting the soundness of this approach (Supplementary Figure 4). Analysis of *TLX1* and *TLX3* connected genes in this setting identified 325 candidate TLX target genes (Fig. 2a), including 70 TLX1- and TLX3- highly significant ($P < 0.0001$) ChIP-chip target genes (Chi-square $P = 0.02$) (Fig. 2b) and 117 genes differentially expressed ($P < 0.0001$) in *TLX1*- and *TLX3*- T-ALLs (Chi-square $P < 0.001$) (Fig. 2c).

Next, we defined the TLX-subnetwork (TLXi) as the space of the T-ALLi encompassing the 445 TLX1- and TLX3- direct target genes (ChIP-chip $P < 0.0001$) that are also differentially expressed in *TLX1*- and *TLX3*-expressing T-ALLs ($P < 0.0001$) and their most direct interconnections (Fig. 3a). The TLXi subnetwork retains the topological features of the

TALLi. Thus, 411/445 (92%) of the genes were involved in at least one interaction, but only 8/445 (< 2%) showed 50 or more direct interactions (Fig. 3b)(Supplementary Table 4). Notably, and consistent with the role of TLX1 as transcriptional repressor TLXi genes transcripts were also characteristically downregulated by GSEA in a transgenic mouse model of TLX1-induced T-ALL[11] (Supplementary Figure 5). Moreover, GSEA analysis of the expression signatures induced by shRNA knockdown of TLX1 in ALL-SIL cells and of TLX3 in the HPB-ALL cell line demonstrated a high level of enrichment of genes in the TLXi among the transcripts upregulated upon inactivation of TLX1 and TLX3 respectively (Supplementary Figures 6 and 7).

Based on these results we proposed that the hierarchical regulatory structure of the TLXi subnetwork could reflect, at least in part, the functional hierarchy of TLX1- and TLX3-target genes involved in T-cell transformation. In this context, *RUNX1*, a critical transcription factor in hematopietic development[12] frequently mutated in acute myeloid leukemias[13-15] stood up as the single most highly interconnected hub in the TLXi (Fig.3b,c). ChIP analysis of TLX1 and TLX3 confirmed the binding of these transcription factors binding to the *RUNX1* promoter (Supplementary Fig. 8). In addition, *RUNX1* was significantly more interconnected in the TLXi-subnetwork than in the T-ALLi as a whole (Chi-square $P = 2.14\times10^{-133}$) and stood up as one of the most prominent TLXi genes downregulated in mouse TLX1-induced T-ALLs (Supplementary Figure 5). Consistently, Master Regulator Analysis [16,17] identified RUNX1 as one of the top most prominent master regulators of the transcriptional program associated with human TLX1 and TLX3 induced leukemias (Supplementary Table 5). The model that emerges from this analysis is a regulatory feedforward loop in which downregulation of RUNX1 by TLX1 and TLX3 would subsequently affect the expression of numerous other TLX target genes (Supplementary Fig. 9). To test this possibility we performed ChIP-chip analysis of RUNX1 direct targets in HPB-ALL cells. In this analysis we identified 308 high confidence RUNX1 target genes ($P < 0.0001$) (Supplementary Table 6). Strikingly, and in concordance with our network analysis, 50% of RUNX1 occupied promoters were also bound by TLX1 and TLX3 (Chi-square $P < 10^{-15}$). Moreover, GSEA analysis of RUNX1 direct target genes showed a high level of enrichment of RUNX1 targets among the top transcripts downregulated in T-ALL cells expressing high levels of *TLX1* or *TLX3* ($P = 0.05$) (Fig. 3d).

These results suggest that *RUNX1* could mediate, at least in part, some of the oncogenic effects of *TLX1* and *TLX3* overexpression. Consistent with this hypothesis, retroviral expression of RUNX1 in TLX1-positive (ALL-SIL) and TLX3 positive (HPB-ALL) cells resulted in impaired cell growth (Supplementary Figure 10) indicating a possible tumor suppressor role for *RUNX1* in T-ALL. Mutation analysis of *RUNX1* in T-ALL revealed the presence of *RUNX1* mutations in 4/12 (33.3%) T-ALL cell lines and 5/114 (4.4%) T-ALL primary samples (Fig. 4a, Supplementary Tables 7 and 8). Interestingly, all ALLs identified in kindreds with FPDMM (platelet disorder, familiar, with associated myeloid malignancy, MIM ID #601399), a leukemia predisposition syndrome caused by mutations in *RUNX1*, happen to be T-ALLs [18-20].

RUNX1 mutations found in T-ALL were heterozygous frameshift truncating mutations (3/10) and missense single nucleotide changes (6/10) (Fig. 4a,b). Notably, DNA sequence

analysis of samples obtained at the time of clinical remission demonstrated the somatic origin of *RUNX1* mutations in each of the 2 cases with available material (Fig. 4b). Moreover, five of these *RUNX1* mutant alleles (pL29S, pH58N, pH78Y, pS114fs and pG138fs) have been previously described as oncogenic mutations in myeloid tumors [21-25]. Interestingly, all four *RUNX1*-mutated samples with available immunophenotype data showed a CD4 and CD8 double negative immunophenotype indicative of a very early arrest in T-cell maturation (Supplementary Table 9). Mapping of T-ALL *RUNX1* mutations on the structure of the RUNX1 runt domain (PDB 1H9D) showed clustering of these amino acid substitutions in the DNA recognition interface of RUNX1 (Fig 4.c). Most strikingly, the RUNX1 H78 residue resides within a highly structurally conserved 16.9 Å diameter cavity frequently targeted by RUNX1 AML mutant alleles, which is adjacent to the DNA binding interface and is predicted to be disrupted in the RUNX1 H78Y T-ALL mutant (Fig 4.c). Next we tested the functional significance of the RUNX1 mutants predicted to be most structurally disruptive in luciferase reporter assays. In these experiments RUNX1 H78Y, RUNX1 S114fs and RUNX1 G138fs showed marked (5 fold) reductions in their capacity to activate a RUNX1-responsive CSF promoter reporter construct compared with wild type RUNX1(Fig. 4d).

Next we analyzed the transcriptional programs and disease kinetics of leukemias occurring in Lck-*TLX1* transgenic *Runx1* wild type mice and in Lck-*TLX1 Runx1* heterozygous knockout animals. This analysis revealed that *TLX1 Runx1* +/+ and *TLX1 Runx1*+/− share a common gene expression program consisting of 215 commonly differentially expressed genes (fold change > 2, P <0.001). However, and consistent with the presence of 50% non overlapping target genes between RUNX1 and TLX1, loss of one copy of *Runx1* partially changes the transcriptional signature of *TLX1*-induced leukemias resulting in 540 differentially expressed transcripts between *TLX1 Runx1*+/+ and *TLX1 Runx1*+/− tumors (fold change > 2, P <0.001) (Supplementary Figure 11). Notably, and despite these transcriptional differences, Lck-*TLX1* transgenic *Runx1* wild type and Lck-*TLX1 Runx1* haploinsuficient mice developed T-ALL with identical kinetics (Supplementary Fig. 12), suggesting that, in agreement with the prediction of our network analysis, the oncogenic effects of *TLX1* are overlapping with the tumor suppressor activity of *Runx1*.

Overall, the integrative analyses presented here (Supplementary Figure 13) show a high level of functional overlap between *TLX1* and *TLX3* in T-cell transformation and identify *RUNX1* as a tumor suppressor gene in T-ALL. Notably, this work highlights the power network analysis to decipher the structure of complex oncogenic circuitries and to identify critical genes and pathways involved in the pathogenesis of human cancer. Moreover, reverse engineering of signaling and transcriptional networks controlling phenotypes associated with distinct gene expression signatures such as cell transformation, metastatic potential or drug resistance could be exploited to identify new therapeutic targets.

METHODS

Clinical samples

Leukemic DNA and cryopreserved lymphoblast samples were provided by collaborating institutions in the US [Eastern Oncology Group (ECOG) and Pediatric Oncology Group

(POG)]. All samples were collected under the supervision of local IRB committees. Informed consent was obtained from all patients at trial entry according to the declaration of Helsinki.

Master Regulator Analysis

Master Regulators (MRs) Analysis was carried out as previously described[16]. Briefly, each set of transcription factor targets (regulon) was partitioned in positive and negative based on the correlation of the transcription factor and target. Positive and negative regulons were tested for enrichment in the TLX1 and TLX3 signature. Redundancy in inferred master regulators that have a large number of common targets was corrected for by removing "shadowed transcription factors", identified as those master regulators whose enrichment is significantly reduced when the common targets are disregarded.

ChIP and ChIP-chip analysis

ChIP-chip analysis of *TLX3* and *RUNX1* target genes was performed in the HPB-ALL cell line. Briefly, 1×10^8 cells were used for chromatin immunoprecipitation using the A-17 goat polyclonal (sc-23397) and the H-55 rabbit polyclonal (sc-30185) antibodies recognizing *TLX3* (Santa Cruz Biotechnology) or two rabbit polyclonal antibodies against RUNX1 (Ab980 from Abcam and 4336S from Cell Signaling Technologies). ChIP-chip was performed following standard protocols provided by Agilent Technologies using Agilent Human Proximal Promoter Microarrays (244K features/array) as previously described [26]. This platform analyzes ~17,000 of the best-defined human genes sourced from UCSC hg18 (NCBI Build 36.1, March 2006) and covers regions expanding from −5.5 kb upstream to +2.5 kb downstream of their transcriptional start sites. We scanned the arrays with an Agilent scanner and extracted the data using the Feature Extraction 8 software. TLX3 and RUNX1 direct target genes were identified using ChIP-chip Significance Analysis (CSA) as described before[26]. MYC and TLX1 ChIP-chip analysis in T-ALL have been previously reported[11,26].

Relative real-time PCR quantitation of *RUNX1* promoter sequences was normalized to *ACTB* gene levels in chromatin immunoprecipitates performed with an antibodies against *TLX1* (C-18 rabbit polyclonal antibody (sc-880), Santa Cruz Biotechnology) and *TLX3* (A-17 goat polyclonal (sc-23397), Santa Cruz Biotechnology) . Primer sequences are listed in Supplementary Table 9.

Reverse engineering of the T-ALL transcriptional networks

To generate a T-ALL transcriptional network we processed Human U133 Plus2.0 Affymetrix microarray gene expression data from a series of 228 T-ALL primary samples using GC-RMA normalization ARACNe algorithm as described before[10] and named the resulting global T-ALL transcriptional network the T-ALL interactome (T-ALLi). Given the high level of overlap between TLX1 and TLX3 regulated direct target genes, and to avoid that the connections between genes showing high levels of mutual information with both TLX1 and TLX3 are eliminated by ARACNe during the Data Processing Inequality step aimed to filter out indirect connections, the expression of these two transcription factors was analyzed as a single node by assigning the same gene label (TLX) to TLX1 or TLX3 probes.

In a separate analysis, we defined the genes experimentally identified as *TLX1*- and *TLX3*-direct targets by ChIP-chip ($P < 0.0001$) and differentially expressed in *TLX1*- and *TLX3*-expressing tumors (differential expression $P < 0.0001$) as the core of the oncogenic program controlled by TLX1 and TLX3 in T-ALL. We then defined the TLX subnetwork (TLXi) as the subspace within the T-ALLi containing all these *TLX1*- and *TLX3*- differentially expressed direct target genes and their shortest path interconnections. The significance of the TLXi was tested performing in silico simulations of 10,000 random networks characterized by the same TLXi features (48 transcription factors and 1,655 connections). The significance of TLXi versus the random generated networks was obtained calculating a non parametric *P* value.

RUNX1 mutation analysis

All *RUNX1* exon sequences were amplified from genomic DNA by PCR and analyzed by direct dideoxynucleotide sequencing. PCR and sequencing primer sequences are listed in Supplementary Table 10.

Structural depiction and analysis

Structural coverage of the RUNX1 protein was identified through use of the PSI-Blast and SKAN algorithms; viable structures were subsequently mapped to all RUNX1 isoforms, and analyzed with the MarkUS web annotation server [27]. Protein database (PDB) structures 1EAN, 1EAO, 1EAQ, 1H9D, 1IO4, 1HJB, 1HJC, and 2J6W were structurally aligned along the RUNX1 Runt domain-DNA interface, and the resulting composite structure was subsequently analyzed to assess conformational flexibilities[28]. Potential effects for the RUNX1 T-ALL mutations were investigated with SCREEN and VASP for cavity prediction and volumetric rendering, ConSurf for analysis of structural conservation, PredUS for protein-protein interface prediction, and DelPhi for highlighting potential alterations in electrostatic potential [27]. Probalistic classification of mutations through physical and evolutionary comparative considerations was conducted through use of the PolyPhen-2 batch servers and algorithms[29]. RUNX1 AML mutations were extracted from the COSMIC database, filtered, and mapped to RUNT domain structures[28]. All structural images were created using UCSF Chimera[28]

Statistical analysis

Significant overlapping between different groups of genes was calculated with the Chi-square test.

Supplementary Material

Refer to Web version on PubMed Central for supplementary material.

ACKNOWLEDGEMENTS

This work was supported by the National Institutes of Health (grants R01CA120196 and R01CA129382 to A.A.F.; and U24 CA114737 to E.P.), the New York Community Trust (A.A.F.), the Innovative Research Award by the Stand Up to Cancer Foundation (A.A.F.), the ECOG tumor bank, the Leukemia & Lymphoma Society Scholar Award (A.F.), the Stichting Kinderen Kankervrij (KiKa; grant 2007-012) (J.P.M) and the Dutch Cancer Society (KWF-EMCR 2006-3500)(J.P.M). A. P. G. is a postdoctoral researcher funded by the Rally Foundation. G.D.G.

was supported by a Marie Curie International Outgoing fellowship. We thank S. Nimer for the pCDNA3 *RUNX1* expression vector, D. Zhang for the pM-CSF-R-luc and the pCMV CBFB plasmids and J. Downing for *Runx1* knockout mice.

REFERENCES

1. Ferrando AA, et al. Gene expression signatures define novel oncogenic pathways in T cell acute lymphoblastic leukemia. Cancer Cell. 2002; 1:75–87. [PubMed: 12086890]
2. Aifantis I, Raetz E, Buonamici S. Molecular pathogenesis of T-cell leukaemia and lymphoma. Nat Rev Immunol. 2008; 8:380–390. [PubMed: 18421304]
3. Hatano M, Roberts CW, Minden M, Crist WM, Korsmeyer SJ. Deregulation of a homeobox gene, HOX11, by the t(10;14) in T cell leukemia. Science. 1991; 253:79–82. [PubMed: 1676542]
4. Kennedy MA, et al. HOX11, a homeobox-containing T-cell oncogene on human chromosome 10q24. Proc Natl Acad Sci U S A. 1991; 88:8900–8904. [PubMed: 1681546]
5. Bernard OA, et al. A new recurrent and specific cryptic translocation, t(5;14)(q35;q32), is associated with expression of the Hox11L2 gene in T acute lymphoblastic leukemia. Leukemia. 2001; 15:1495–1504. [PubMed: 11587205]
6. Van Vlierberghe P, et al. The recurrent SET-NUP214 fusion as a new HOXA activation mechanism in pediatric T-cell acute lymphoblastic leukemia. Blood. 2008; 111:4668–4680. [PubMed: 18299449]
7. Ferrando AA, et al. Prognostic importance of TLX1 (HOX11) oncogene expression in adults with T-cell acute lymphoblastic leukaemia. Lancet. 2004; 363:535–536. [PubMed: 14975618]
8. Su XY, et al. Various types of rearrangements target TLX3 locus in T-cell acute lymphoblastic leukemia. Genes Chromosomes Cancer. 2004; 41:243–249. [PubMed: 15334547]
9. Basso K, et al. Reverse engineering of regulatory networks in human B cells. Nat Genet. 2005; 37:382–390. [PubMed: 15778709]
10. Margolin AA, et al. ARACNE: An Algorithm for the Reconstruction of Gene Regulatory Networks in a Mammalian Cellular Context. BMC Bioinformatics. 2006; 7(Suppl 1):S1–7.
11. De Keersmaecker K, et al. The TLX1 oncogene drives aneuploidy in T cell transformation. Nat Med. 2010; 16:1321–1327. [PubMed: 20972433]
12. Speck NA, Gilliland DG. Core-binding factors in haematopoiesis and leukaemia. Nat Rev Cancer. 2002; 2:502–513. [PubMed: 12094236]
13. Song WJ, et al. Haploinsufficiency of CBFA2 causes familial thrombocytopenia with propensity to develop acute myelogenous leukaemia. Nat Genet. 1999; 23:166–175. [PubMed: 10508512]
14. Osato M, Yanagida M, Shigesada K, Ito Y. Point mutations of the RUNx1/AML1 gene in sporadic and familial myeloid leukemias. Int J Hematol. 2001; 74:245–251. [PubMed: 11721958]
15. Osato M. Point mutations in the RUNX1/AML1 gene: another actor in RUNX leukemia. Oncogene. 2004; 23:4284–4296. [PubMed: 15156185]
16. Lefebvre C, et al. A human B-cell interactome identifies MYB and FOXM1 as master regulators of proliferation in germinal centers. Mol Syst Biol. 6:377. [PubMed: 20531406]
17. Carro MS, et al. The transcriptional network for mesenchymal transformation of brain tumours. Nature. 463:318–325. [PubMed: 20032975]
18. Preudhomme C, et al. High frequency of RUNX1 biallelic alteration in acute myeloid leukemia secondary to familial platelet disorder. Blood. 2009; 113:5583–5587. [PubMed: 19357396]
19. Owen CJ, et al. Five new pedigrees with inherited RUNX1 mutations causing familial platelet disorder with propensity to myeloid malignancy. Blood. 2008; 112:4639–4645. [PubMed: 18723428]
20. Nishimoto N, et al. T cell acute lymphoblastic leukemia arising from familial platelet disorder. Int J Hematol. 92:194–197. [PubMed: 20549580]
21. Osato M, et al. Biallelic and heterozygous point mutations in the runt domain of the AML1/PEBP2alphaB gene associated with myeloblastic leukemias. Blood. 1999; 93:1817–1824. [PubMed: 10068652]

22. Rocquain J, et al. Combined mutations of ASXL1, CBL, FLT3, IDH1, IDH2, JAK2, KRAS, NPM1, NRAS, RUNX1, TET2 and WT1 genes in myelodysplastic syndromes and acute myeloid leukemias. BMC Cancer. 10:401. [PubMed: 20678218]

23. Langabeer SE, Gale RE, Rollinson SJ, Morgan GJ, Linch DC. Mutations of the AML1 gene in acute myeloid leukemia of FAB types M0 and M7. Genes Chromosomes Cancer. 2002; 34:24–32. [PubMed: 11921279]

24. Auewarakul CU, et al. AML1 mutation and its coexistence with different transcription factor gene families in de novo acute myeloid leukemia (AML): redundancy or synergism. Haematologica. 2007; 92:861–862. [PubMed: 17550866]

25. Christiansen DH, Andersen MK, Pedersen-Bjergaard J. Mutations of AML1 are common in therapy-related myelodysplasia following therapy with alkylating agents and are significantly associated with deletion or loss of chromosome arm 7q and with subsequent leukemic transformation. Blood. 2004; 104:1474–1481. [PubMed: 15142876]

26. Margolin AA, et al. ChIP-on-chip significance analysis reveals large-scale binding and regulation by human transcription factor oncogenes. Proc Natl Acad Sci U S A. 2009; 106:244–249. [PubMed: 19118200]

27. Fischer M, et al. MarkUs: a server to navigate sequence-structure-function space. Nucleic Acids Res. 39:W357–361. [PubMed: 21672961]

28. Pettersen EF, et al. UCSF Chimera--a visualization system for exploratory research and analysis. J Comput Chem. 2004; 25:1605–1612. [PubMed: 15264254]

29. Adzhubei IA, et al. A method and server for predicting damaging missense mutations. Nat Methods. 7:248–249. [PubMed: 20354512]

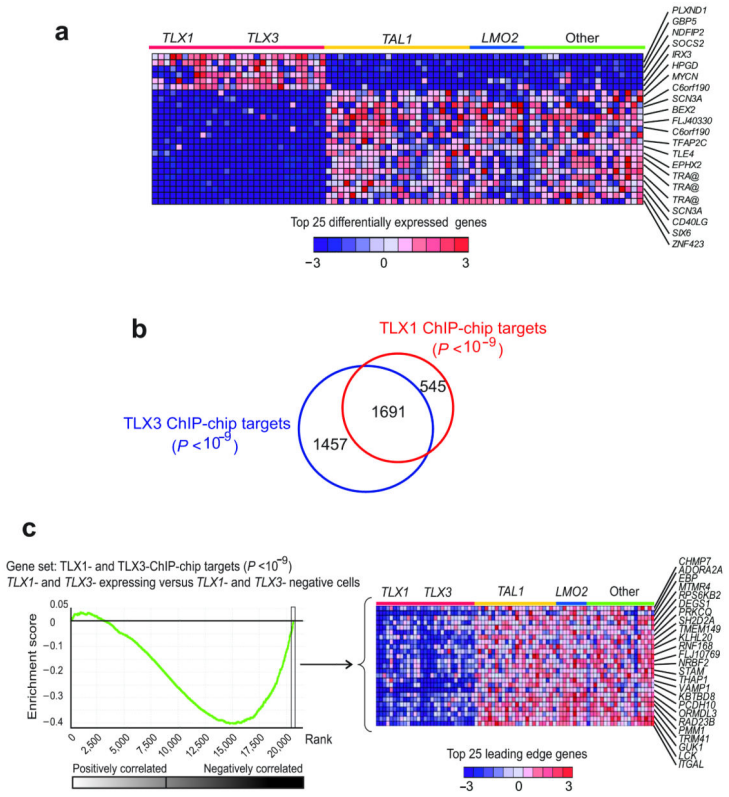

Figure 1. *TLX1*- and *TLX3*-expressing T-ALLs are associated with a distinct gene expression signature highly enriched in downregulated TLX1- and TLX3-ChIP-chip direct target genes

(**a**) Heat map representation of the top 25 differentially expressed genes ($P < 0.005$; Fold change > 2) in *TLX1*- and *TLX3*-expressing T-ALLs. (**b**) Venn diagram representation showing the overlap between *TLX1* and *TLX3* ChIP-chip direct target genes (**c**) GSEA analysis of TLX1 and TLX3 ChIP-chip direct target genes in *TLX1*- and *TLX3*-expressing T-ALLs. Enrichment plots (left) and heat map representations of the 25 top ranking genes in the leading edge (right) are shown. Genes in heat maps are shown in rows, each individual sample is shown in one column. The scale bar shows color coded differential expression from the mean in standard deviation units with red indicating higher levels and blue lower levels of expression.

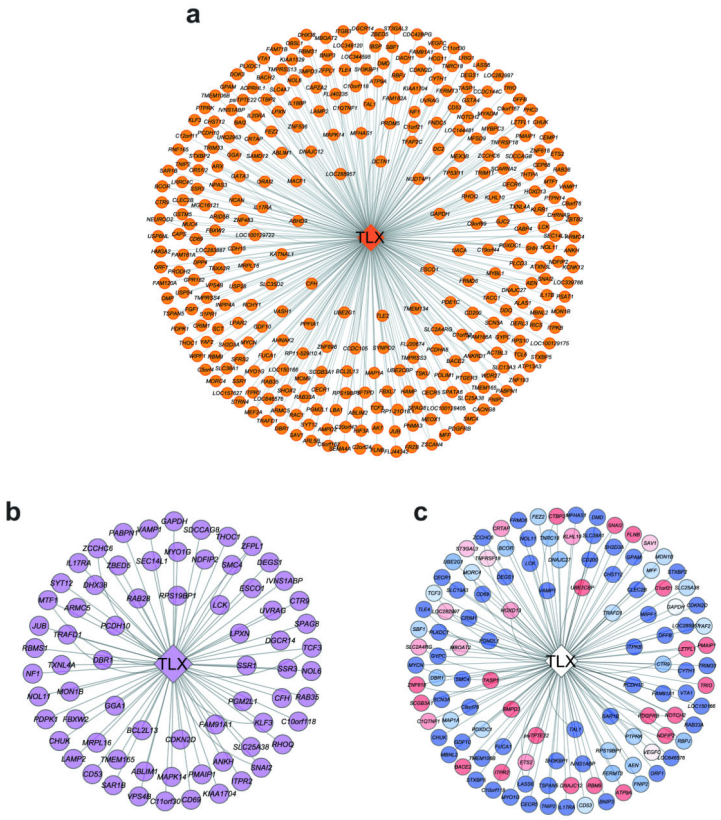

Figure 2. An ARACNe transcriptional network identifies TLX1- and TLX3-direct targets and *TLX1*- and *TLX3*- differentially expressed genes

(**a**) Graphic representation of node first neighbors in the T-ALLi ARACNe transcriptional network connected to a *TLX1* and *TLX3* metagene (TLX). (**b**) TLX first neighbor genes in the ARACNe transcriptional network identified as *TLX1*- and *TLX3*-ChIP-chip direct target genes (ChIP-chip $P < 0.0001$). (**c**) TLX first neighbor genes in the ARACNe transcriptional network differentially expressed in *TLX1*- and *TLX3*-expressing T-ALLs (Differential expression $P < 0.0001$). Relative expression in *TLX1*- and *TLX3*-expressing T-ALLs is color coded with nodes in red indicating upregulated and nodes blue indicating downregulated genes.

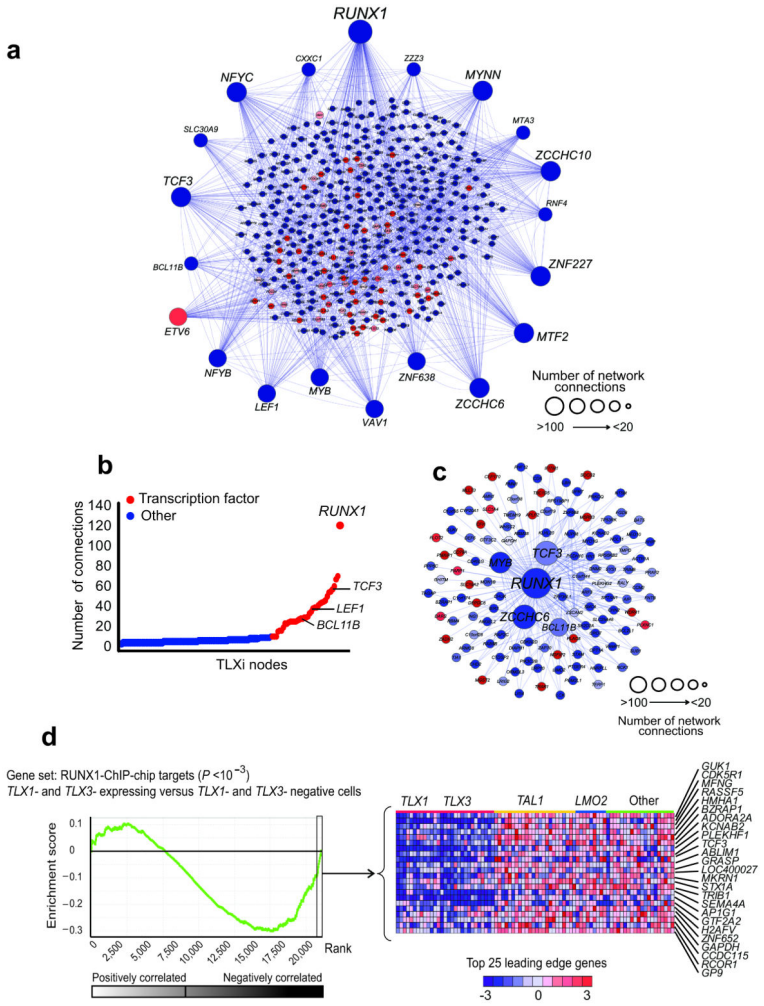

Figure 3. Reverse engineering and structure analysis of the TLXi subnetwork

(**a**) Graphic representation of the TLXi subnetwork. Each node represents a *TLX1*- and *TLX3*- ChIP-chip direct target ($P < 0.0001$) gene differentially expressed ($P < 0.0001$) in *TLX1*- and *TLX3*-expressing T-ALLs. (**b**) Connectivity plot representing the connections of each gene within the TLXi. Transcription factors are colored in red and non transcription factor encoding genes are indicated in blue (**c**) Sun diagram showing the *RUNX1* first neighbor genes in the TLXi. Relative expression in *TLX1*- and *TLX3*-expressing T-ALLs is color coded in the network representation with nodes in red indicating upregulated and nodes blue indicating downregulated genes. (**d**) GSEA analysis of RUNX1 ChIP-chip direct target genes in *TLX1*- and *TLX3*-expressing T-ALLs. Enrichment plots (left) and heat map representations of the 25 top ranking genes in the leading edge (right) are shown. Genes in heat maps are shown in rows, each individual sample is shown in one column. The scale bar shows color coded differential expression from the mean in standard deviation units with red indicating higher levels and blue lower levels of expression.

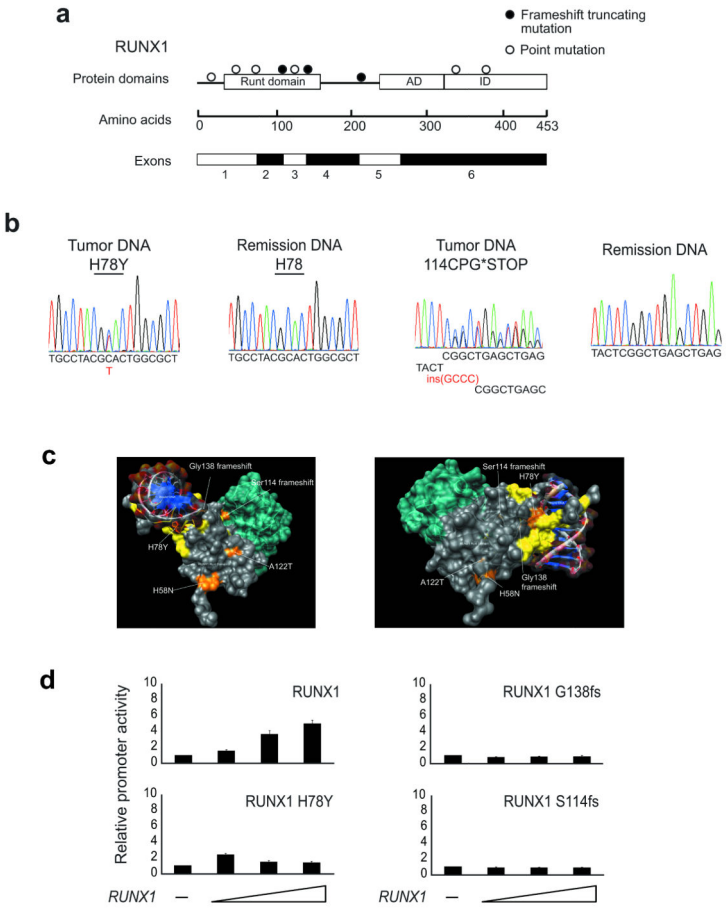

Figure 4. *RUNX1* mutations in T-ALL

(**a**) Schematic representation of *RUNX1* mutations identified in T-ALL. Runt: *RUNX1* DNA binding domain; AD: activation domain; ID: inhibitory domain (**b**) Representative DNA sequencing chromatograms of paired diagnostic and remission genomic DNA T-ALL samples showing somatically acquired mutations in the *RUNX1* gene. (**c**) Molecular surface rendition depicting the interaction between the RUNX1 runt domain (grey), DNA and CBFB (green) complex. RUNX1 mutations present in T-ALL and AML are indicated in orange. RUNX1 mutations found in AML are depicted in yellow. (**d**) Effects of *RUNX1* T-ALL mutant alleles in the activity of a CSF promoter reporter construct. The size of the nodes in the star diagrams is proportional to the significance *P* value as indicated in the scale at the bottom.